Properties of the upper part of the last glacial loess-palaeosol sequence at Savudrija (Istria, Croatia)

Hećej, Nina; Durn, Goran

6th Regional Scientific Meeting on Quaternary Geology: Seas, Lakes and Rivers
Ljubljana, Slovenia

28th September 2021

Properties of the upper part of the Last Glacial loess-palaeosol sequence at Savudrija (Istria, Croatia)

NINA HEĆEJ & GORAN DURN

INTRODUCTION

- **Fieldwork**
- 7,5 m thick loess-palaeosol sequence in Savudrija, Istria (CRO)
- performed within NALPS (*engl. North Adriatic Loess-Paleosol Sequences*) project

- **Reason for the survey?**
- To investigate the **origin, age** and **features of the six horizons** (depth 0-205 cm) located in the upper part of the loess-palaeosol sequence from Istria, Croatia
- **How?**
- By applying detailed mineralogical, geochemical, pedophysical and micromorphological analyzes
- + OSL dating

GEOGRAPHICAL POSITION AND GEOLOGY OF THE RESEARCHED AREA

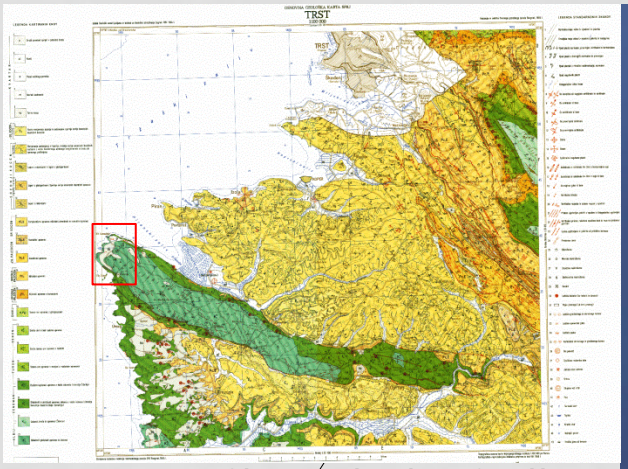

Figure 2. *A crop of the Basic Geological Map of Republic of Croatia, 1:100000 Trst sheet*

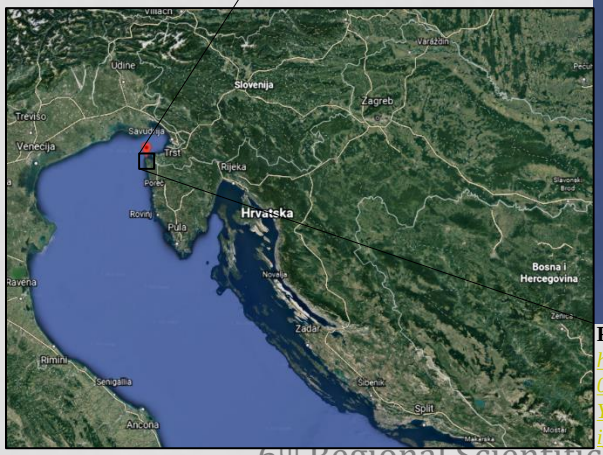

Figure 1. *Geographical position of Savudrija profile (modified after https://earth.google.com/web/search/Savudrija/@45.01709433,14.29590456,5.54042896a,199229.65405215d,35y,-0h,0t,0r/data=CmIaOBIyCiUweDQ3N2I3Yjk1YzczMmNkYTk6MHgyNjAwYWQ1MTUzMzZlNzgyKglTYXZ1ZHJpamEYASABIiYKJAluNcT3wlNIQBG1ywFYPANFQBlNdNoQOVw4QCHMSaBxhegOQA?utm_source=earth7&utm_campaign=vine&hl=hr)*

Figure 3. *a) Profile through pedosedimentary complex with shown sampling sites; b) the investigated part of the pedosedimentary complex*

FIELDWORK RESULTS

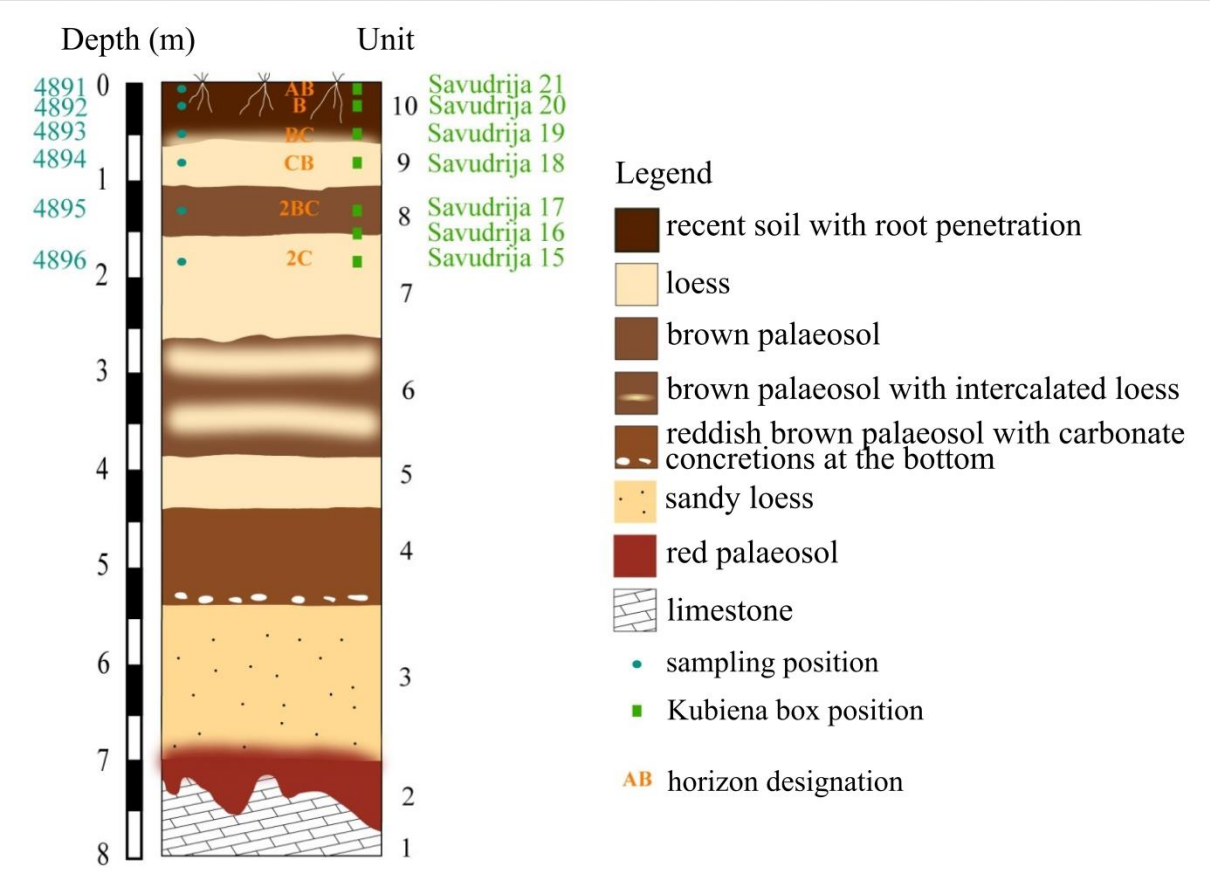

Munsell's color chart:

•4891 : 7,5 YR 5/3 (brown)

Other samples's hues: 10 YR (light-brown to yellowish-brown)
•color: goethite

Figure 4. *The graphical log of the Savudrija loess-palaeosol sequence with indicated sampling positions analyzed within this thesis (modified after ZHANG et al., 2018)*

LABORATORY WORK

- detailed chemical analysis
- physical and chemical analysis of the paleosols (incl. CEC and base saturation, particle size analysis, analysis of iron and manganese oxides and hydroxides soluble in dithionite-citrate bicarbonate and oxalate)
- mineral composition analysis (XRD method)
- optically and infrared stimulated luminescence (OSL & IRSL)
- micromorphological analysis of thin sections.

Table 4. Chemical properties of the upper part of the Savudrija profile

Sample ID	Horizon	pH		Description	$CaCO_3$ [%]	Description	Humus [%]	Description	Organski C (%humus/ 1,72) [%]	Total C[%]	Organic C (Total C - anorganic C) [%]
		H_2O	KCl								
4891	AB	8,22	7,38	alkaline	1,7	Low carbonate content	2,53	Low humosity	1,47	2,05	1,85
4892	B	8,87	7,30	alkaline	7,4	Low carbonate content	2,79	Low humosity	1,62	1,57	0,69
4893	BC	9,14	7,53	alkaline	24,8	Medium carbonate content	4,91	Medium humosity	2,85	3,85	0,87
4894	CB	9,20	7,58	alkaline	34,7	High carbonate content	2,77	Low humosity	1,61	5,24	1,08
4895	2BC	8,58	7,59	alkaline	27,5	High carbonate content	5,82	High humosity	3,38	4,37	1,06
4896	2C	8,39	7,65	alkaline	36,1	High carbonate content	2,40	Low humosity	1,40	5,54	1,20

CATION EXCHANGE CAPACITY (CEC) & PERCENT BASE SATURATION (BS)

Table 6. CEC values of the upper part of the Savudrija profile

CEC = b(Mg) + b(Na) + b(K) + b(Ca) [meq/100g]		
Sample	**b(Mg) + b(Na) + b(K) + b(Ca)**	**RSD [%]**
4891	79,954	0,8805
4892	87,661	1,0857
4893	107,811	1,3056
4894	138,861	1,1542
4895	147,626	1,7274
4896	142,318	1,3447

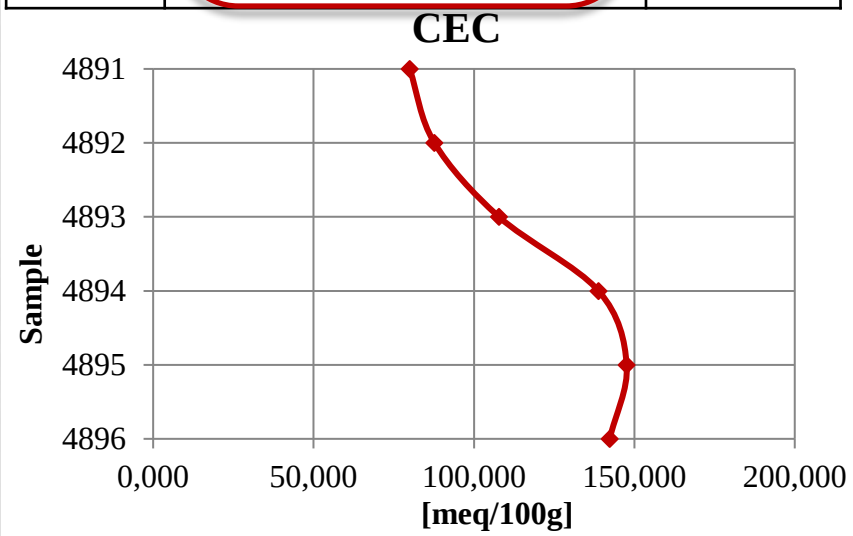

Figure 9. *CEC values by profile depth*

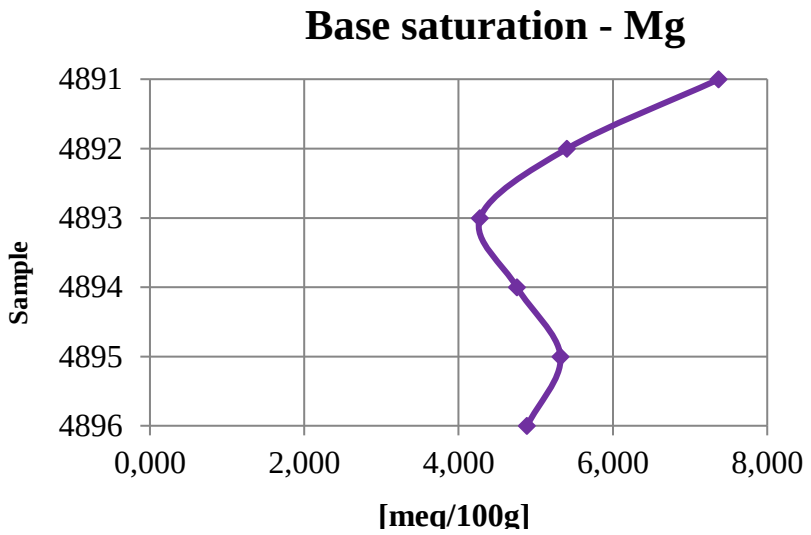

Figure 7 . *Percent base saturation of Mg2+*

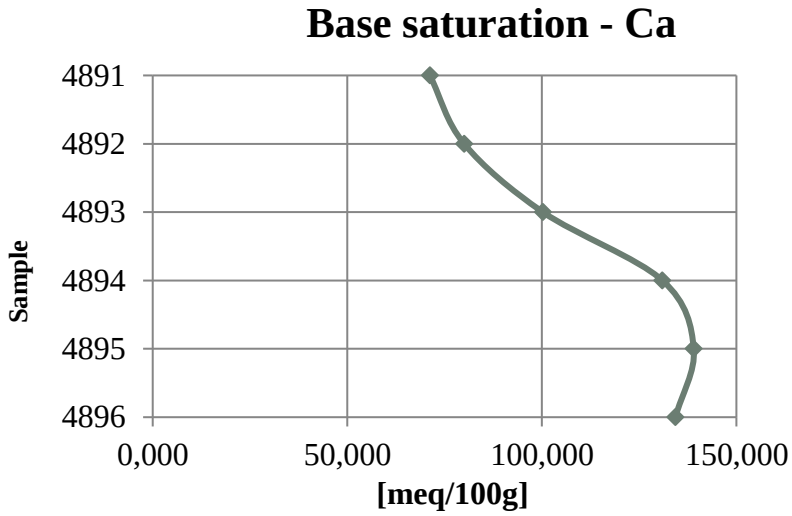

Figure 8. *Percent base saturation of Ca2+*

GEOCHEMICAL RATIOS

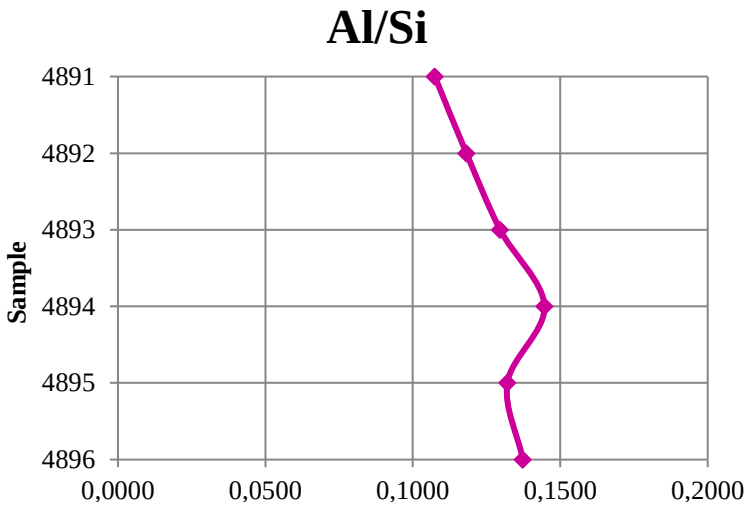

Figure 10. *Al/Si ratio by depth*

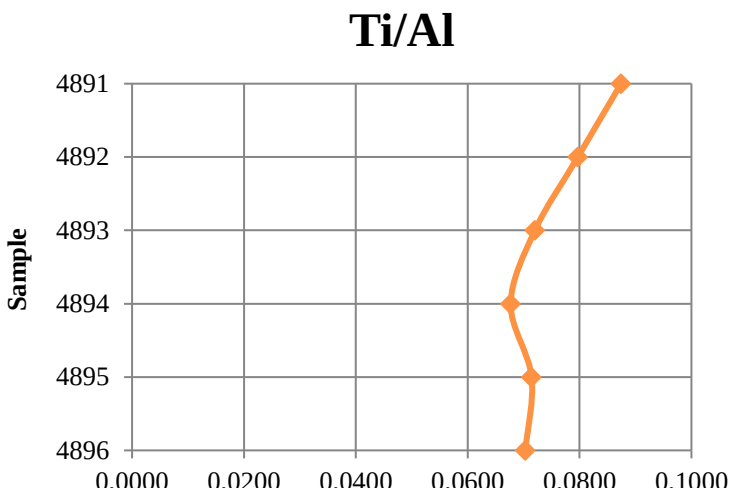

Figure 11. *Ti/Al ratio by depth*

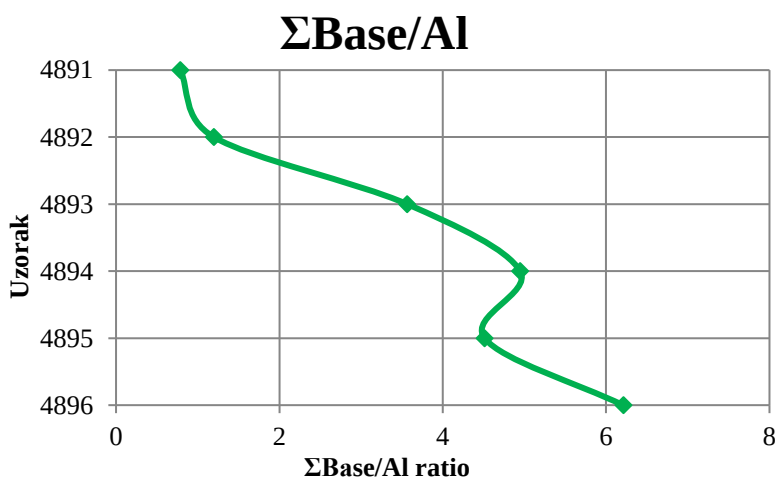

Figure 12. *ΣBase/Al ratio by depth*

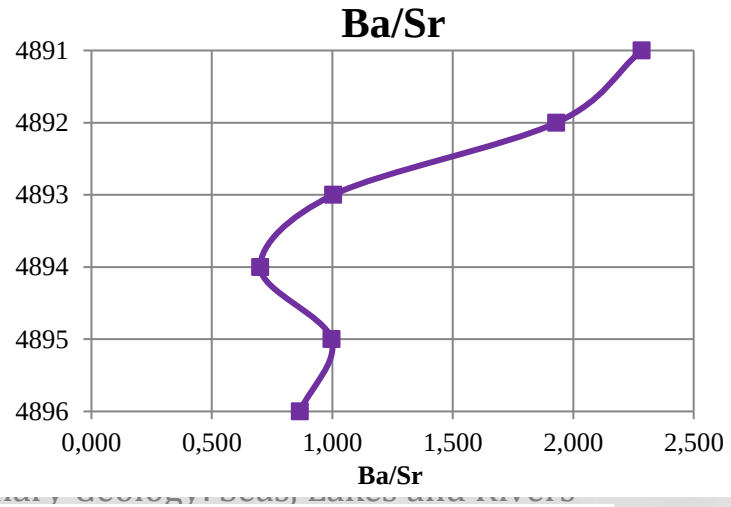

Figure 13. *Ba/Sr ratio by depth*

DCB & OXALATE SOLUBLE IRON

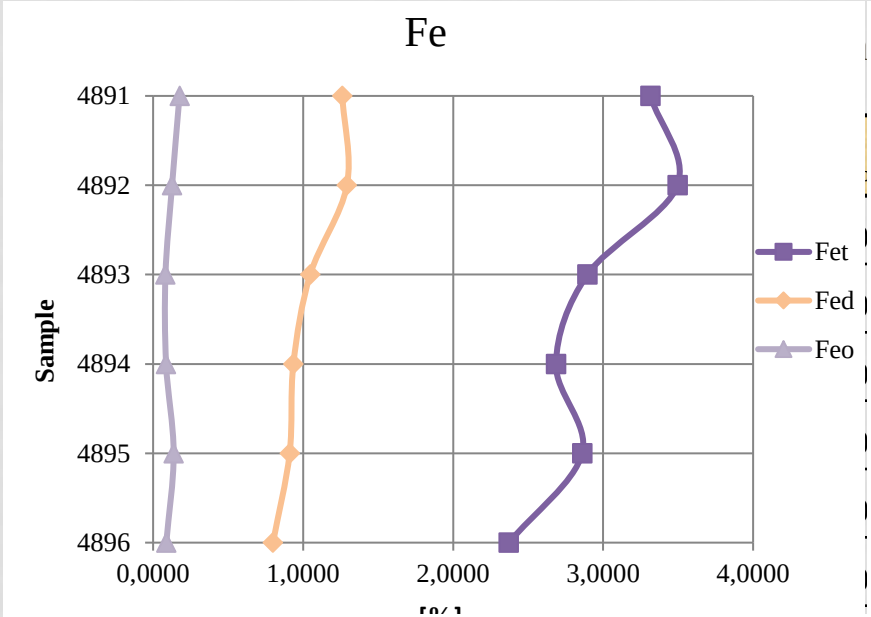

Figure 14. *total (Fet), dithionite-soluble (Fed) and oxalate soluble ((Feo) iron per profile depth*

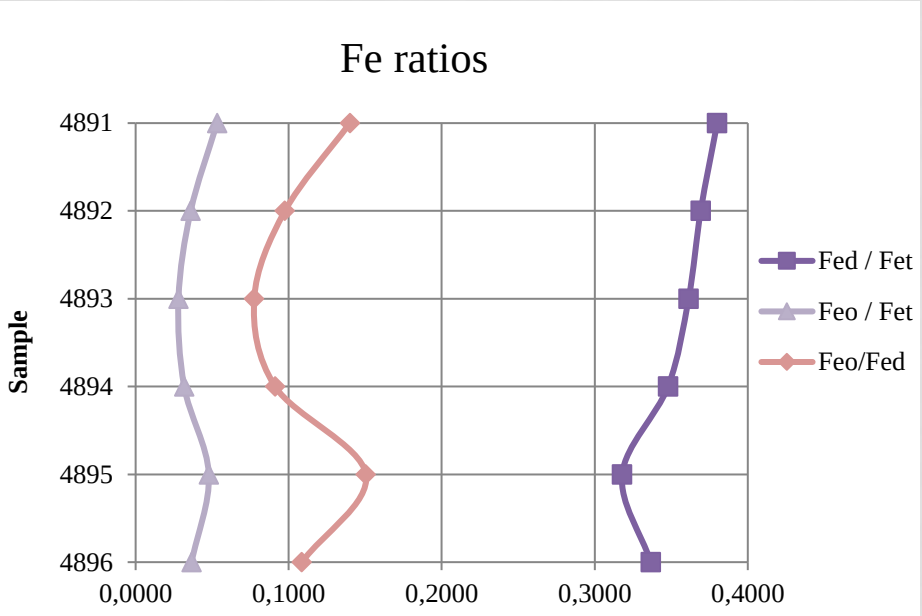

Figure 15. *Ratios of total (Fet), dithionite-soluble (Fed) and oxalate soluble ((Feo) iron per profile depth*

- The mean value of the Fe_d / Fe_t ratio is 0.35, which according to ARDUINO et al. (1984) & DURN (1996), indicate a medium degree of weathering.

DCB & OXALATE SOLUBLE MANGANESE

- **Table 9.** Shares and ratios of total (Mn_t), dithionite-soluble (Mn_d) & oxalate soluble Mn (Mn_o).

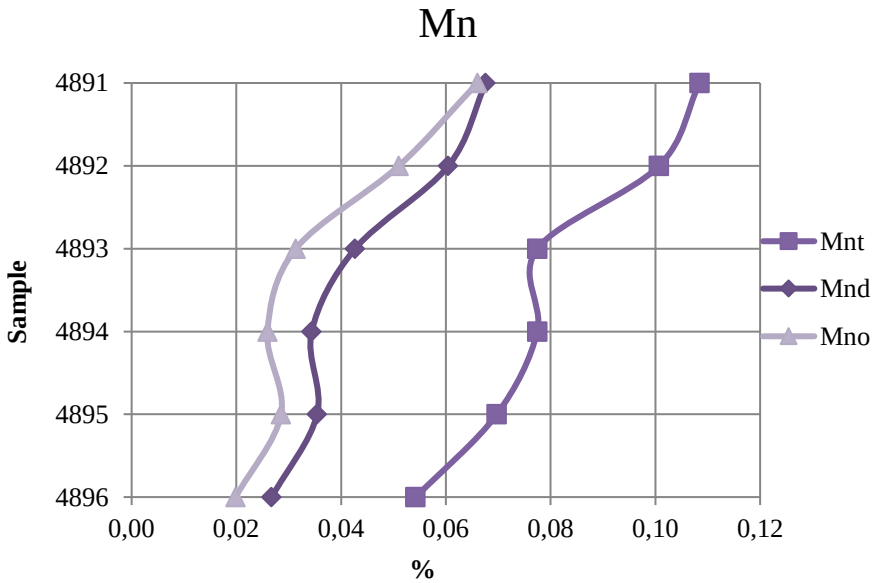

Figure 16. *Total (Mnt), dithionite-soluble (Mnd) and oxalate (Mno) soluble manganese by profile depth*

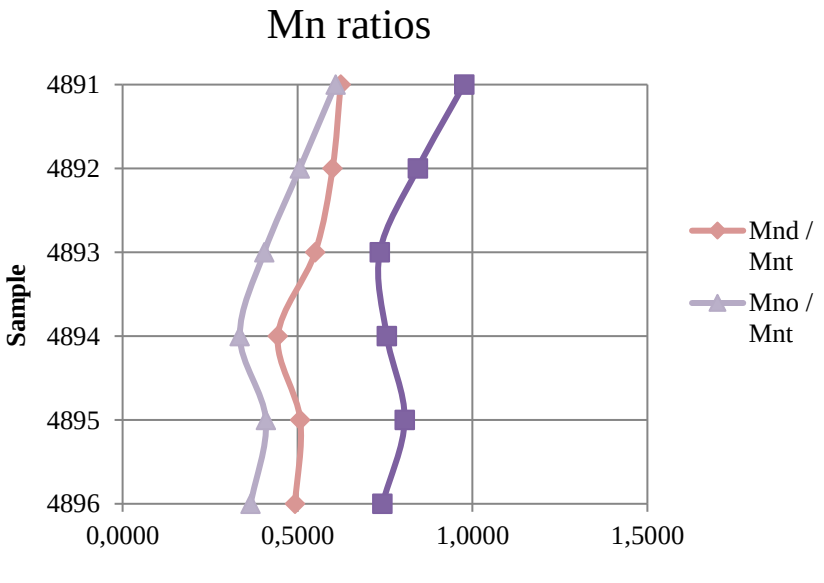

Figure 17. *Ratios of total (Mnt), dithionite-soluble (Mnd) and oxalate soluble (Mno) manganese per profile depth*

MODAL COMPOSITION

Table 12. Semiquantitative mineral composition of the clay fraction (particle size & <2μm) of samples after dissolution of carbonate (in wt %).

Sample	Clay component	Qtz	Pl	Kfs	Gt	Hm	Amph	Ill	Kln	Chl	14Å		Chl - Vrm	MM / NIM	AC
											S	Vrm			
4891 <2μm	25,90	6	+	?	+	-/?	?	++	+/++	++	++ (S i/ili Vrm)		+/++	+++	+
4892 <2μm	31,10	5	-	-	+	?	-	++	++	+/++	+/++	?	+/++	++/+++	+
4893 <2μm	26,30	5	-	-	+	?	-	++	++	+/++	++ (S i/ili Vrm)		+/++	++/+++	+
4894 <2μm	23,90	6	-	-	+	-	-	++	++	+/++	++ (S i/ili Vrm)		+/++	++/+++	+
4895 <2μm	21,40	7	-	-	+	-	-	++	++	++	?	++	?	++/+++	+/++
4896 <2μm	20,60	5	-	-	+	-	-	++	++	+/++	?	?	? (Chl -Ill)	++/+++	+/++

OSL & IRSL AGE

Table 13. OSL and IRSL ages of the upper part of the section

Sample ID	Lab ID	Depth [cm]	IRSL age [ka]	OSL age [ka]
SAV 7	4894	55 - 115	17,5 ± 1,2	8,9 ± 0,6
SAV 6	4896	165 - 205	31,4 ± 2,5	20,4 ± 1,6

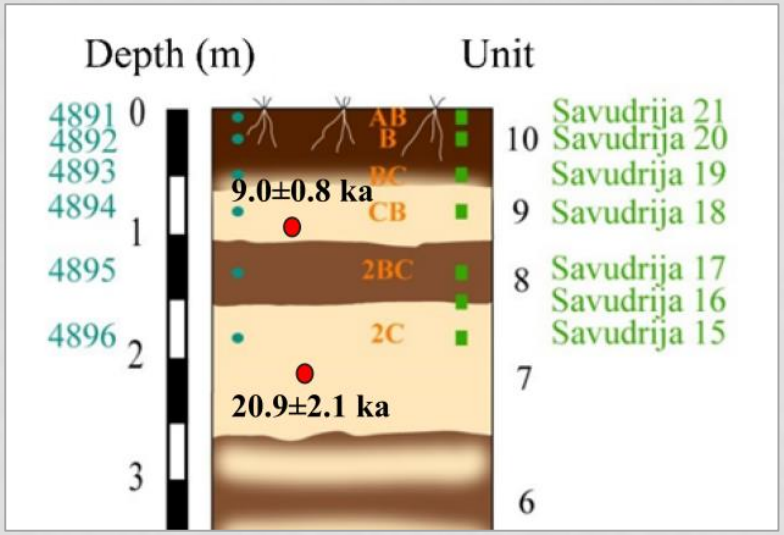

Figure 18. The graphical log of the upper part of Savudrija loess-palaeosol sequence OSL and IRSL ages of the two loess horizons (modified after ZHANG et al., 2018)

MICROMORPHOLOGICAL FEATURES

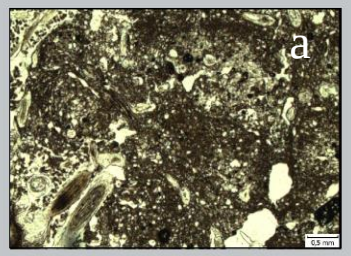

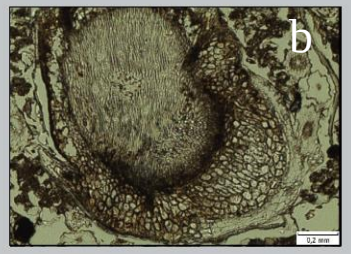

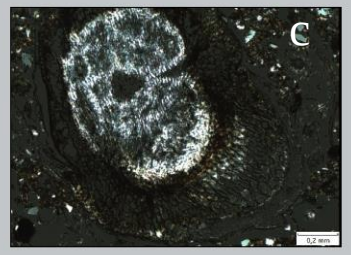

***Figure 19**. Thin section Savudrija 21; **a)** c / f distribution in the thin section; pedofeatures: rhizoconcretions within voids and cracks, Fe/Mn oxide nodules , accumulation of dispersed organic matter(PPL); **b)** Rhizoconcretion (dimension 1,25 mm) with a pronounced honeycomb structure filled with secondary carbonate: **b)** (PPL); **c)** (XPL)*

Savudrija 21

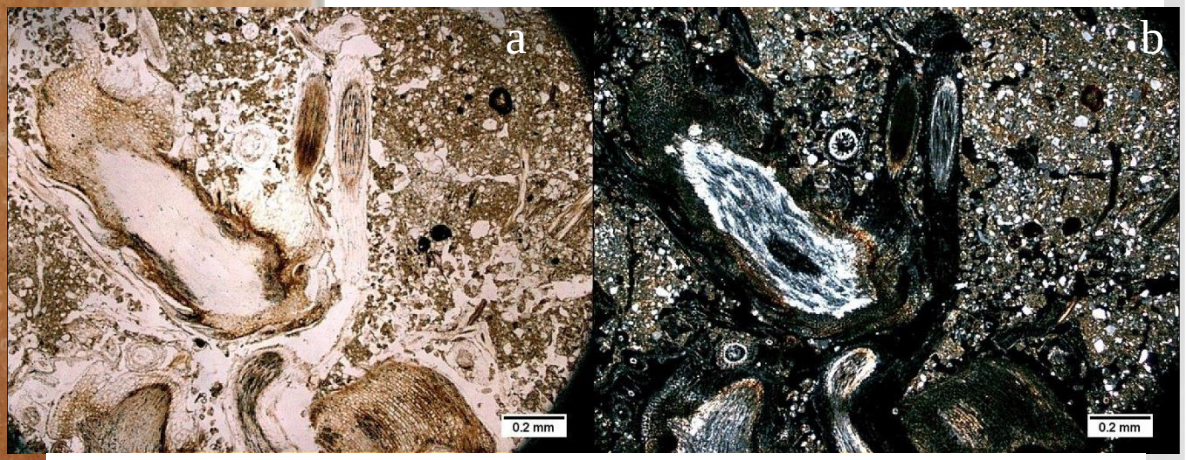

***Figure 20**. Savudrija 21: crystallisation of calcite in the internal part of the plant cell wall) **a)** PPL; **b)** XPL*

MICROMORPHOLOGICAL FEATURES

Savudrija 20

-**microstructure:** spongy/vesicular
-**pedofeatures**: dominant rhizoliths, with Fe- &Mn nodules, few pedorelicts (brown coloured well-rounded forms)
-**pedality**: weak, with predominantly angular grains and poor sorting

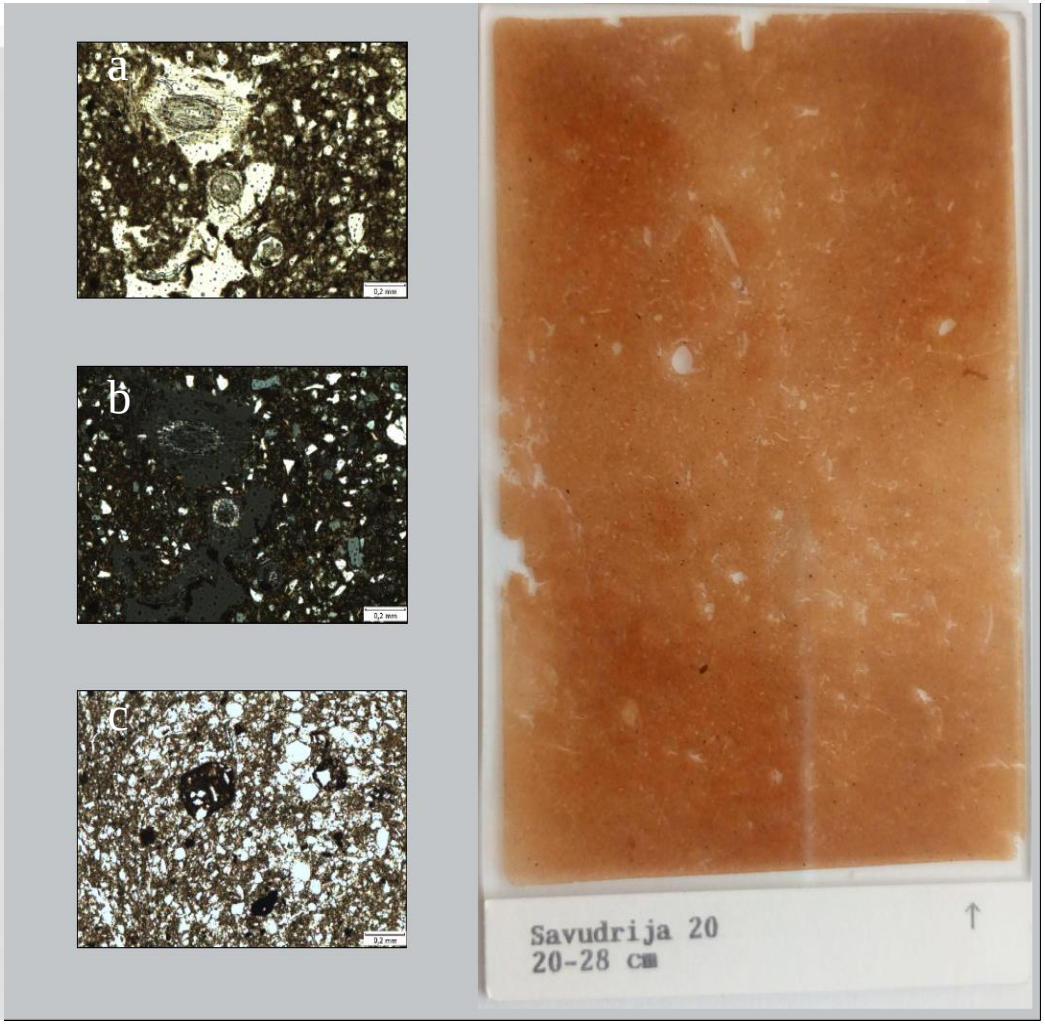

Figure 21. *Savudrija 20;* ***a)*** *rhizoliths with secondary crystallised calcite within voids (PPL);* ***b))*** *rhizoliths with secondary crystallised calcite within voids (XPL);* ***c)*** *Fe-Mn nodules with embedded Qtz-grains (PPL)*

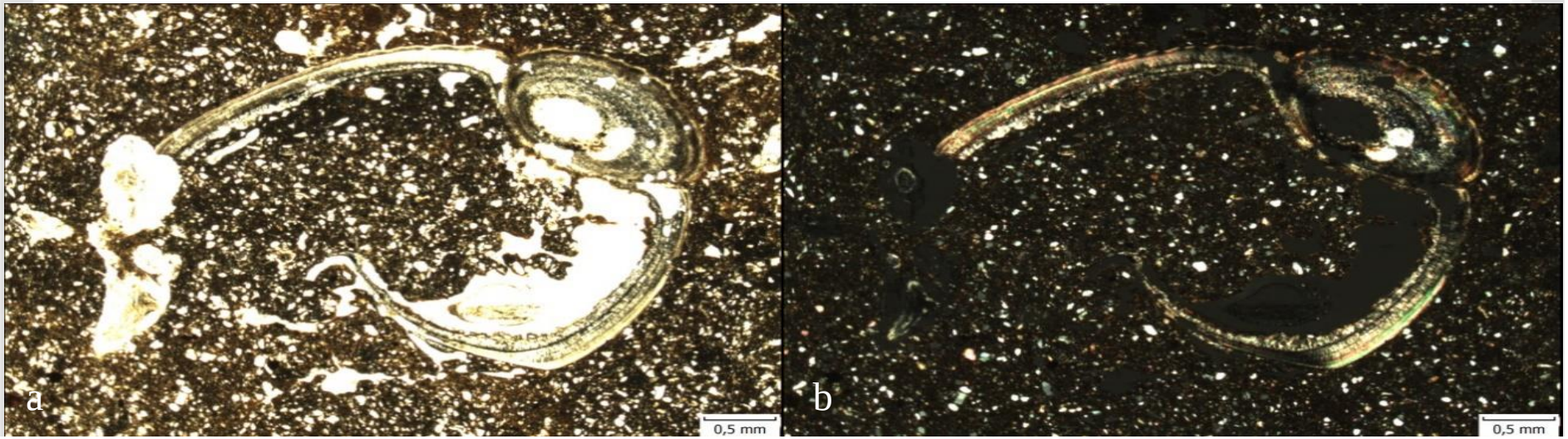

Figure 23 . *Savudrija 19: axial cross section of the brachiopod shell (PPL & XPL*

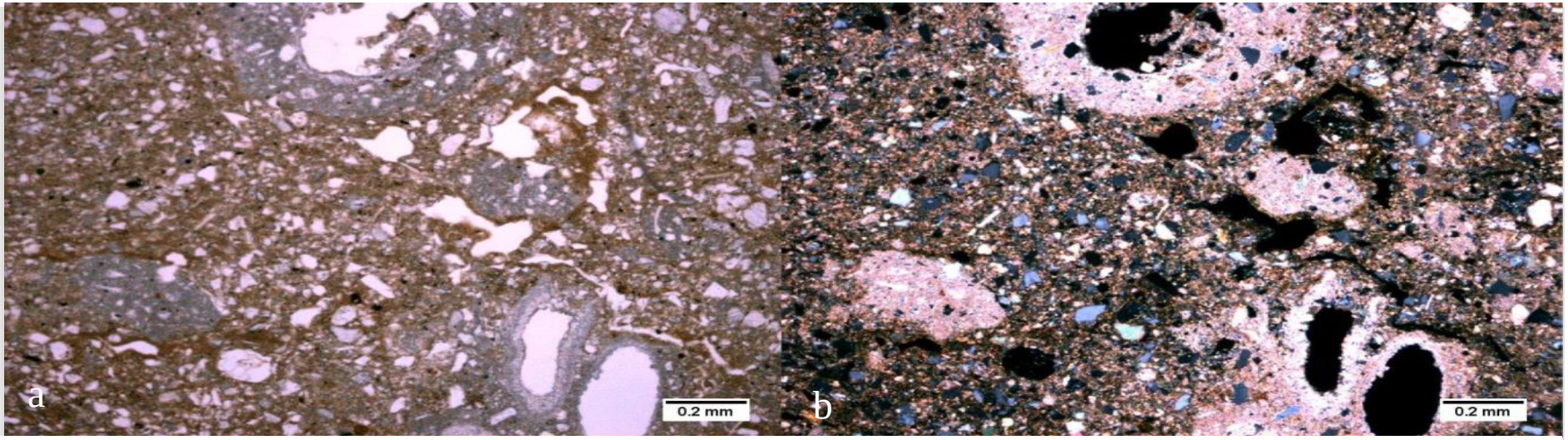

Figure 24. *Accumulation of rhizoconcretions and chain aggregation of secondary carbonates along the edges of the cavities (PPL & XPL)*

MICROMORPHOLOGICAL FEATURES

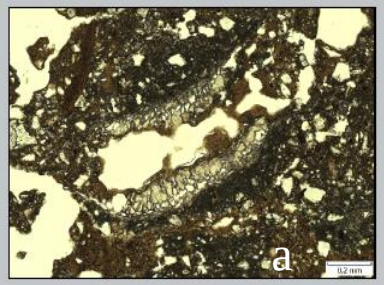

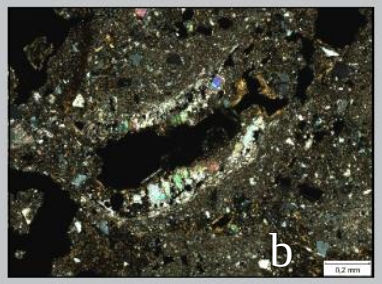

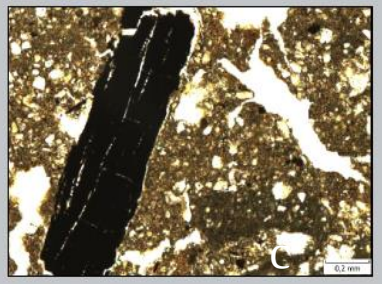

Savudrija 18

-**microstructure:** chanelly with *vughs*

- **pedofeatures:** clay coatings, Fe & Mn nodules, aglomeration of secondary crystalised calcite, higher amount of organic matter

-**pedality:** weak, with angular to rounded aggregates; in lower part of the section stronger bioturbation is observed

Figure 25. *Thin section Savudrija 18;* ***a)*** *crystallized agglomerated grains of secondary calcite and clay coating along the edge of the crack (PPL),* ***b)*** *crystallized agglomerated grains of secondary calcite and clay coating along the edge of the crack (XPL),* ***c)*** *An elongated fragment of charcoal (PPL)*

MICROMORPHOLOGICAL FEATURES

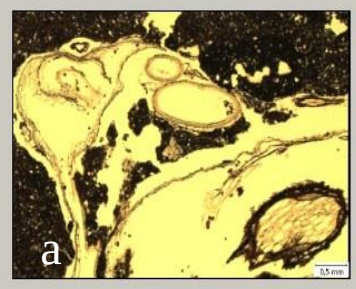

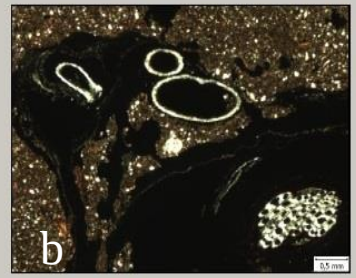

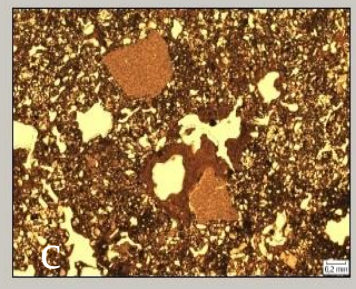

Savudrija 17

-**microstructure:** channelly to spongy

-**pedofeatures**: clay and calcite coatings, replacement of quartzite grain with calcite, abundance of Fe/Mn oxide noduls, rhizocretions

Higher amount of organic matter

-**pedality:** weak, with angular to rounded aggregates

Figure 26. *accumulation of dispersed organic matter, christalization of secondary calcite along the mollusc shell fragments in thin section Savudrija 17* ***a)*** *(PPL),* ***b*** *(XPL)*

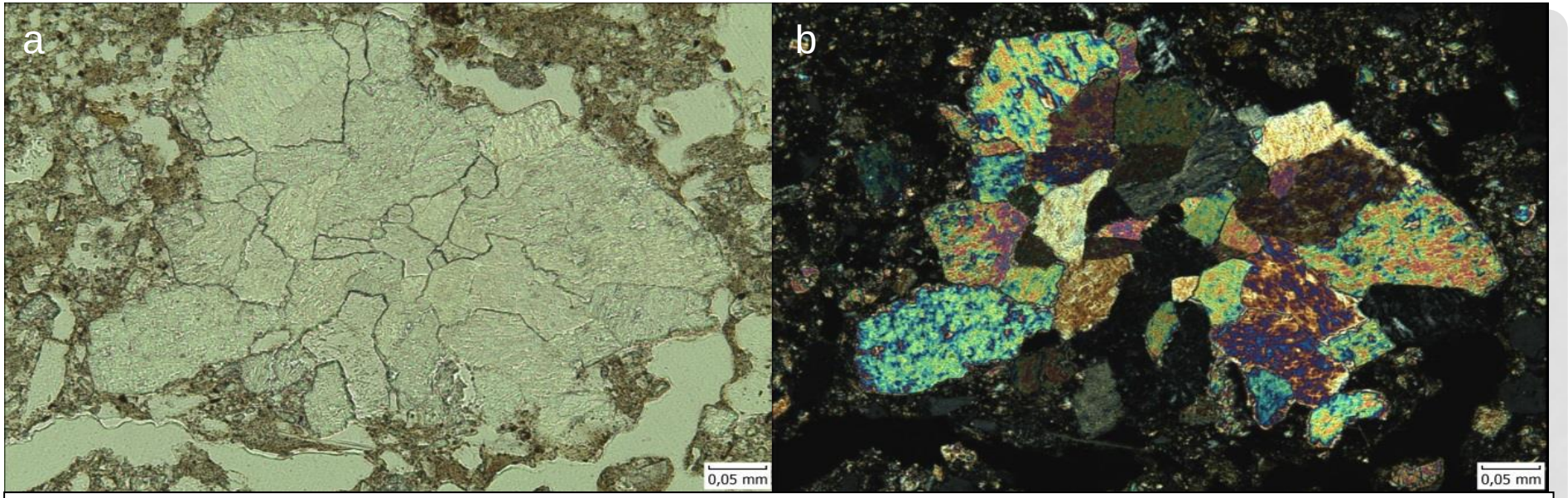

Slika 26. a) *replacement of chert grain with calcite (PPL),* ***b)*** *replacement of chert grain with calcite(XPL) observed in thin section Savudrija 17*

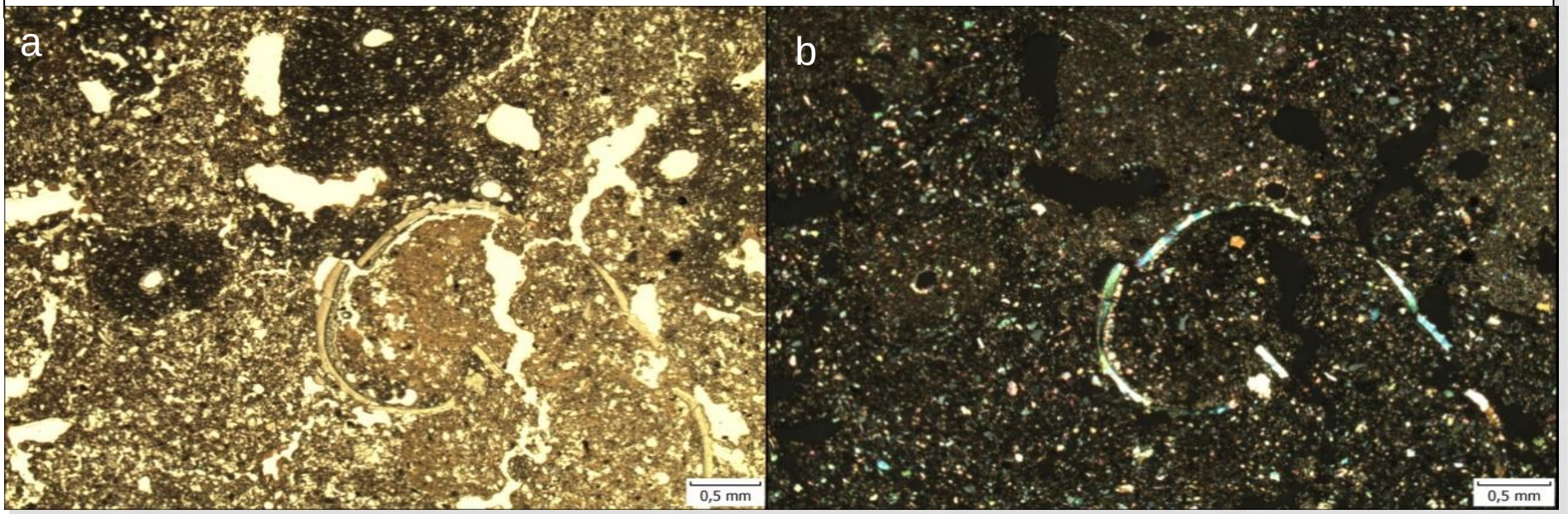

Figure 27. *Pedofeatures observed in thin section Savudrija 17;* ***a)*** *Rhizoconcretions with observed crystalization of calcite along the cell wall (PPL),* ***b)*** *Rhizocretions with observed crystalization of calcite along the cell wall (XPL)*

MICROMORPHOLOGICAL FEATURES

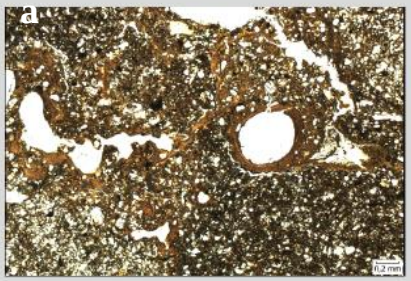

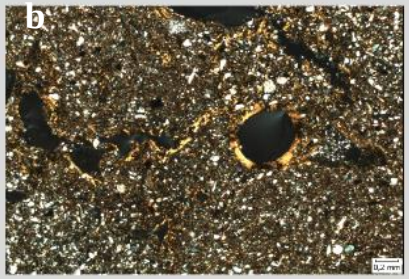

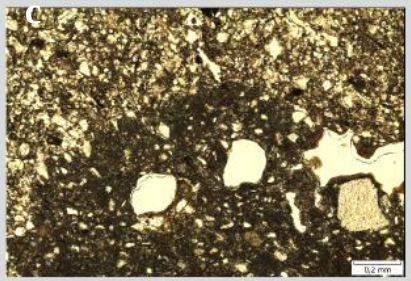

Savudrija 16

-**microstructure:** spongy with *vughs* and channels

-**pedofeatures**: clay coatings, Fe/Mn oxide nodules and secondary crystalized calcite

- replacement of chert grain with calcite; molluscs shell fragments observed

-high amount of organic matter

-**pedality**: weak to medium

Figure 28. *Savudrija 16;* ***a)*** *dispersed organic matter and clay coatings along the edge of cracks and cavities (PPL),* ***b)*** *(XPL),* ***c)*** *Dispersed organic matter in contact with the grain of chert (PPL),*

MICROMORPHOLOGICAL FEATURES

Savudrija 15

-**microstructure**: spongy to *vughy*-channelly

- **pedofeatures** : Fe-Mn oxide nodules, a lot of clay coatings; agglomerated grains of sekundary crystalized calcite

-**pedality**: weak to medium

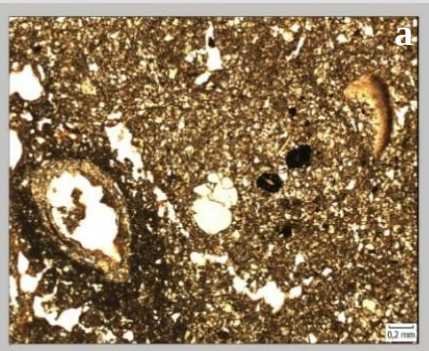

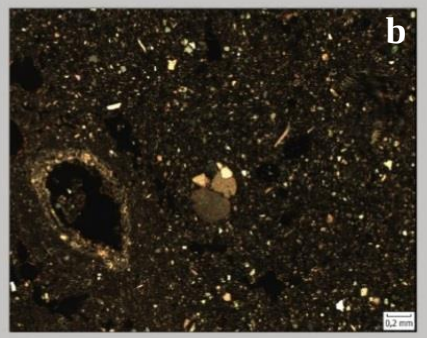

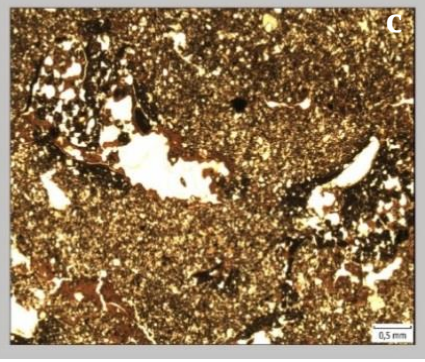

Figure 29. *Pedofeatures observed in thin section Savudrija 15;* ***a)*** *dispersed organic matter, accumulation of clay coatings along the edge of the channel and vughs, rounded dark brown to black Fe - Mn nodules, nodules of agglomerated calcite and secondary crystallized calcite within the shell fragments (PPL);* ***b)*** *(XPL);* ***c)*** *dispersed organic matter and clay coatings along the edge of vughs (PPL)*

CONCLUSION

- The uppermost part of the sequence studied was represented by presumably polygenetic soil developed on loess (AB-B-BC-CB) underlain by brown palaeosol developed on older loess (2BC-2C). Based on the Sm/Nd and La/Ce geochemical ratios (SHELDON & TABOR, 2009), it was also determined that the loess parent material examined in this study has the same provenance as the materials examined in BANIČEK (2016) and DURN et al. (2018a, b).
- XRD analysis revealed that all soil samples contain a significant amount of quartz, plagioclase, alkali feldspar, illitic material, kaolinite, chlorite, 14 Å minerals (vermiculite and/or smectite), mostly irregular mixed-layer clay minerals, goethite and amorphous components, whose content increases with depth.
- Based on quartz OSL dating, the age of the studied soil horizon CB is 9 ± 0.8 ka and of soil horizon 2C is 20.9 ± 2.1 ka (ZHANG et al., 2018).
- Micromorphological studies of the uppermost part of the section revealed two superimposed loess substrates in which (palaeo)sols developed. significant share of rhizoconcretions, ferrous/manganese oxide nodules and clay coatings, which indicate that there have been a significant illuviation in the horizons of the uppermost part of the Savudrija pedosediment complex.

As part of the research preparation, this work has been supported in part by the Croatian Science Foundation under the projects ACCENT (3274) and WIANLab (8054)